

Variation of muonic x-ray spectra with electronic structure: A study of iron compounds

R. A. Naumann,* H. Daniel, P. Ehrhart, F. J. Hartmann, and T. von Egidy
 Physik-Department, Technische Universität München, D-8046 Garching, West Germany
 (Received 23 July 1984)

The *K* series of muonic x rays of iron has been measured from FeCl_3 , Fe_2O_3 , $\text{K}_3\text{Fe}(\text{CN})_6$, and aqueous solutions of $\text{Fe}(\text{NO}_3)_3$ and $\text{K}_3\text{Fe}(\text{CN})_6$. Significant differences in the x-ray-intensity pattern were observed and related to the structure of the outer electrons of Fe in these compounds. The influence of the ionic radius and ionic charge and of hydrogen in aqueous solutions is discussed. The importance of open *d*- or *f*-electron configurations is demonstrated.

I. INTRODUCTION

Following the discovery of charged muons, there has been continuing theoretical and experimental interest in the processes occurring when these particles come to a stop in matter. To clarify this in particular for the negative particles, a considerable number of systematic experiments have now been reported where the Coulomb capture of muons in elements or compounds was investigated (cf. Ref. 1 and literature cited therein). These studies amply verified striking features first reported by Zinov *et al.*² and Kessler *et al.*³ in their pioneering investigations both of the muon-capture ratios² for given classes of binary compounds as well as the intensity patterns³ of the mesic-atom x rays emitted after the capture process. It is by now well documented that both the capture ratios and the intensity patterns correlate with the group position of the capturing element in the chemical periodic table. Thus one concludes that the particular electronic-shell structure of the capturing element plays a decisive role in the capture process. There remains, however, the question of which atomic or molecular electrons are primarily responsible for the observed periodicities. One may ask, for

example, "Do only the most loosely bound valence electrons contribute to the observed periodicities?" or "Do these arise from interactions of the muon with the more deeply bound electrons in the inner atomic shells?"

To help answer these questions one may consider experimental data reported for some of the simplest compounds, halides, and oxides of the group-IA, -IIA, and -IIIA elements.

Table I shows corresponding per-atom capture ratios $A(Z, Z')$ recently compiled by von Egidy and Hartmann.¹ An examination of these data shows that, for a given type of compound, there is no large variation in the per-atom capture ratio as the charge on the isoelectronic cations increases across a major row of the periodic table. The data⁴ summarized in Table II indicate that for some of these isoelectronic ions the changes occurring in the ionic radius and the next vacuum ionization potential are large.

Comparing the data of Tables I and II one may conclude that for ionic solids composed of simple ions having a given inert-gas closed-shell electronic configuration, there is little effect on the capture ratio when the nuclear charge is varied. These rather small changes sharply contrast with the major effect of increasing nuclear charge on the total ionic charge, ionization potential, and crystal ra-

TABLE I. Selected experimental per-atom muon-capture ratios $A(Z, Z')$ (as listed in Ref. 1) for cations and anions of atomic numbers Z and Z' , respectively. (For a direct citation of the experimental data, consult Ref. 1.)

Ion	Oxide	Compound Fluoride	Chloride
$^{11}\text{Na}^+$	0.99 ± 0.05 (Na_2O_2)	0.97 ± 0.05 (NaF)	0.79 ± 0.03 (NaCl)
$^{12}\text{Mg}^{+2}$	0.89 ± 0.05 (MgO)	0.92 ± 0.03 (MgF_2)	0.76 ± 0.04 (MgCl_2)
$^{13}\text{Al}^{+3}$	0.74 ± 0.05 (Al_2O_3)	0.95 ± 0.17 (AlF_3)	0.66 ± 0.04 (AlCl_3)
$^{19}\text{K}^+$		1.89 ± 0.19 (KF)	1.14 ± 0.02 (KCl)
$^{20}\text{Ca}^{+2}$		1.47 ± 0.26 (CaF_2)	1.41 ± 0.07 (CaCl_2)
$^{37}\text{Rb}^+$	2.58 ± 0.20 (RbO_2)	2.41 ± 0.18 (RbF)	1.53 ± 0.19 (RbCl)
$^{38}\text{Sr}^{+2}$	2.12 ± 0.11 (SrO)	1.83 ± 0.28 (SrF_2)	
$^{39}\text{Y}^{+3}$	2.19 ± 0.16 (Y_2O_3)	2.54 ± 0.19 (YF_3)	
$^{55}\text{Cs}^+$	3.25 ± 0.26 (CsO_2)	3.65 ± 0.35 (CsF)	2.21 ± 0.23 (CsCl)
$^{56}\text{Ba}^{+2}$	2.84 ± 0.36 (BaO_2)	3.32 ± 0.40 (BaF_2)	2.67 ± 0.33 (BaCl_2)
$^{57}\text{La}^{+3}$	2.73 ± 0.33 (La_2O_3)	3.93 ± 0.28 (LaF_3)	

TABLE II. Selected properties of ions with inert-gas electron configurations (experimental data taken from Ref. 4).

Inert gas	Ion	Ionization potential of ion (eV)	Crystal radius of ion (Å)
Ne	$_{11}\text{Na}^+$	47.3	0.97
	$_{12}\text{Mg}^{+2}$	80.1	0.66
	$_{13}\text{Al}^{+3}$	120.0	0.51
Xe	$_{55}\text{Cs}^+$	25.1	1.67
	$_{56}\text{Ba}^{+2}$	35.5	1.34

dus, a property essentially determined by the outer, most loosely bound electrons.

Additional evidence for the insensitivity of capture ratios to ionic charge or radius comes from per-atom capture ratios measured for two pairs of alkali halides.^{1,5} Each pair contains oppositely charged ions with the same electronic configurations: RbCl versus KBr and CsCl versus KI. The experimental capture ratios are shown in Table III.

Each row of this table compares the capture ratios for ions with closed-shell electron configurations. The first ratio compares the capture of a cation to an anion, the second ratio an anion to a cation. The relative insensitivity to ionic charge (or ionic radius) is striking. These observations are in accordance with recent calculations of capture ratios⁶ which showed that these ratios depend essentially on the electrons bound with less than 80 eV and on Z .

With the data now available one may also compare the muonic x-ray-intensity patterns for compounds and elements containing cations with closed electron major shells. Lyman intensity patterns measured⁷⁻¹³ for Na, Mg, Al; Cl, K, Ca; Rb, Sr; and Cs, Ba are compared in Table IV.

One observes that the muonic x-ray-intensity pattern is insensitive to the charge on the ionic core. In addition, one can note that there is little effect when a given element exists in either a nonconducting ionic salt or as the free metallic element. Apparently presence of an open conduction electron band has little consequence.

The existing data so far cited for isoelectronic systems suggest that structural variations from changing nuclear charge of either the outermost valence electrons or the inner core electrons contained in closed major shells are not responsible for the observed periodicities in the muonic capture process.

Changes in the electron occupation and/or structure of the incomplete d - (and f -) electron shells being filled for the elements located towards the middle of the longer rows of the periodic table (fourth through eighth rows) then remain as the likely cause of this behavior. We decided to test this possibility by searching for possible variations in the muonic Lyman x-ray-intensity pattern for one transition element, iron ($Z = 26$), following capture in a number of different chemical compounds. In these compounds the iron atom has the same formal oxidation state, +3, but for one of these compounds the d -electron structure is known to be markedly different. The systems chosen were anhydrous ferric chloride (FeCl_3), ferric oxide (Fe_2O_3), an aqueous solution of ferric nitrate [$1.9M \text{Fe}(\text{NO}_3)_3$, $3.0M \text{HNO}_3$], and potassium ferricyanide [$\text{K}_3\text{Fe}(\text{CN})_6$] in both crystalline form and a $1.0M$ aqueous solution. In one group are the compounds and one solution where a simple Fe^{+3} ionic structure is expected: FeCl_3 , Fe_2O_3 , $1.9M \text{Fe}(\text{NO}_3)_3$. The second group is the compound and the solution containing the ferricyanide complex, i.e., a negatively charged octahedral molecular complex where the iron is surrounded by six cyanide groups. We also wished to compare the results of these studies with the detailed investigation of the muonic x-ray-intensity pattern for metallic iron earlier reported from this laboratory.¹⁴

II. EXPERIMENT AND RESULTS

The samples were contained in target holders consisting of a polystyrene frame with interior dimensions $0.60 \text{ cm} \times 5.0 \text{ cm} \times 7.0 \text{ cm}$ and top and bottom plates of 0.1-cm thickness. The hygroscopic target of anhydrous FeCl_3 was prepared in a glove box filled with dry argon. The area thickness of the target samples was in the cases of FeCl_3 , 0.40 g/cm^2 ; Fe_2O_3 , 1.0 g/cm^2 ; $1.9M \text{Fe}(\text{NO}_3)_3$,

TABLE III. Ionic electron ratio R and experimental muon-capture ratios $A(Z, Z')$ for isoelectronic simple ionic salts.

$R = 36:18$	RbCl	$A_{(37\text{Rb}, 17\text{Cl})} = \begin{matrix} 1.75 \pm 0.18^a \\ 1.53 \pm 0.19^b \end{matrix}$	$\text{KBr } A_{(35\text{Br}, 19\text{K})} = 1.69 \pm 0.17^a$
$R = 54:18$	CsCl	$A_{(55\text{Cs}, 17\text{Cl})} = \begin{matrix} 2.07 \pm 0.21^a \\ 2.21 \pm 0.23^b \end{matrix}$	$\text{KI } A_{(53\text{I}, 19\text{K})} = 1.85 \pm 0.19^a$

^aExperimental data taken from Ref. 5.

^bExperimental data taken from Ref. 1.

TABLE IV. Experimental K -series intensity patterns for elements and compounds containing closed-shell cations.

Element	Compound	K_α	K_β	K_γ	K_δ	K_ϵ	K_ζ	Reference
^{11}Na	Na	79.5 ± 0.3	8.4 ± 0.2	5.76 ± 0.19	3.81 ± 0.16	1.69 ± 0.12	0.70 ± 0.08	7
	Na	78.6 ± 0.4	8.8 ± 0.2	6.3 ± 0.2	4.4 ± 0.2	1.6 ± 0.2	0.24 ± 0.12	8
	Na_2O_2	77.2 ± 0.4	9.2 ± 0.3	6.0 ± 0.2				9
	NaCl	81.3 ± 0.7	8.1 ± 0.4	5.2 ± 0.3	3.4 ± 0.2	1.5 ± 0.1	0.34 ± 0.06	10
^{12}Mg	Mg	79.6 ± 0.7	7.8 ± 0.3	5.3 ± 0.3	3.73 ± 0.19	2.12 ± 0.14	0.86 ± 0.05	11
	MgO	80.1 ± 0.5	8.2 ± 0.4	5.5 ± 0.3				9
	MgCl_2	81.1 ± 0.8	7.4 ± 0.4	4.8 ± 0.3	3.3 ± 0.2	1.7 ± 0.2	0.9 ± 0.1	10
^{13}Al	Al	79.7 ± 0.6	7.4 ± 0.2	4.7 ± 0.2	3.89 ± 0.17	2.35 ± 0.11	1.13 ± 0.08	11
	Al_2O_3	79.3 ± 0.5	8.0 ± 0.3	4.9 ± 0.3				9
^{19}K	K	84.1 ± 0.4	6.4 ± 0.2	2.27 ± 0.17	1.93 ± 0.17	1.77 ± 0.17	1.26 ± 0.17	8
	KCl	82.6 ± 1.1	6.2 ± 0.5	3.3 ± 0.5	2.0 ± 0.4	2.8 ± 0.4	3.2 ± 0.8	10
	KCl	84.3 ± 0.7	6.2 ± 0.3	2.4 ± 0.2	2.5 ± 0.3	2.2 ± 0.2	1.1 ± 0.3	12
^{20}Ca	Ca	82.8 ± 0.4	6.5 ± 0.2	2.07 ± 0.16	2.07 ± 0.16	2.07 ± 0.16	1.49 ± 0.16	8
	CaO	82.0 ± 0.7	6.3 ± 0.4	2.3 ± 0.2	2.0 ± 0.2	1.7 ± 0.2	1.5 ± 0.2	13
	CaCl_2	81.4 ± 1.2	7.4 ± 0.7	2.3 ± 0.4	2.7 ± 0.5	2.2 ± 0.4	1.5 ± 0.5	10
^{37}Rb	RbO_2	85.3 ± 1.9	5.2 ± 0.4	1.5 ± 0.3	0.6 ± 0.3	0.6 ± 0.3	0.8 ± 0.3	13
^{38}Sr	SrO	85.6 ± 1.9	5.5 ± 0.4	1.8 ± 0.4	1.0 ± 0.3	0.7 ± 0.3	0.8 ± 0.3	13
^{55}Cs	CsO_2	88.2 ± 1.9	5.9 ± 1.0	1.4 ± 0.3	0.4 ± 0.2			13
^{56}Ba	BaO	88.7 ± 1.9	5.3 ± 1.0	1.0 ± 0.3	0.6 ± 0.3			13

0.90 g/cm^2 ; $\text{K}_3\text{Fe}(\text{CN})_6$, 0.72 g/cm^2 ; and $1.0M$ $\text{K}_3\text{Fe}(\text{CN})_6$, 0.68 g/cm^2 .

The muonic Lyman x-ray spectra were recorded at muon channel I of the Swiss Institute for Nuclear Research (SIN), Villigen, Switzerland. A Ge(Li) spectrometer with a sensitive volume of 80 cm^3 was employed.

The spectra were recorded both in prompt and delayed coincidence with a muon stopping telescope and stored in the memory of an on-line computer. As an example, Fig. 1 shows part of the spectrum from solid $\text{K}_3\text{Fe}(\text{CN})_6$.

The muonic K -x-ray intensities for iron were obtained from the observed x-ray lines using computer line fitting,

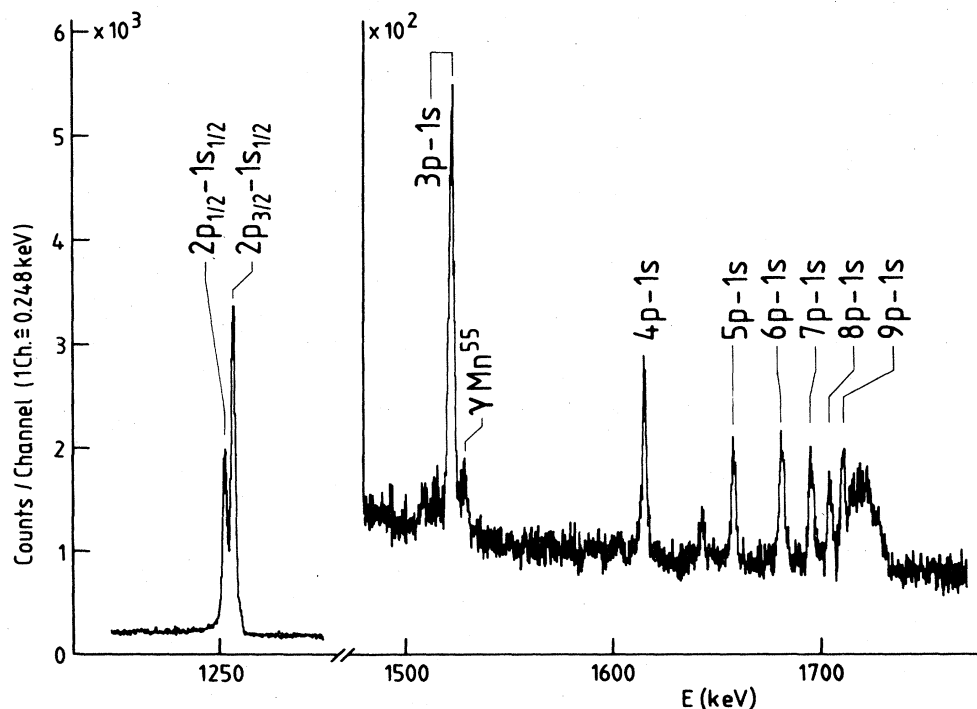


FIG. 1. Part of the muonic x-ray spectrum from solid $\text{K}_3\text{Fe}(\text{CN})_6$.

TABLE V. Experimental muonic K -series intensities ($np \rightarrow 1s$ transitions).

n	FeCl ₃	Fe ₂ O ₃	1.9M Fe(NO ₃) ₃	K ₃ Fe(CN) ₆	1.0M K ₃ Fe(CN) ₆	Fe metal ^a
2	75.29±0.36	74.68±0.70	74.90±0.5	70.14±0.72	68.46±0.56	71.61±1.65
3	7.19±0.16	7.66±0.22	7.70±0.32	7.98±0.39	8.30±0.34	8.17±0.25
4	2.72±0.11	2.61±0.09	2.40±0.16	2.98±0.19	3.11±0.27	2.82±0.12
5	1.66±0.10	1.82±0.10	1.88±0.14	2.27±0.12	2.46±0.25	1.75±0.12
6	2.15±0.12	2.12±0.10	2.23±0.20	2.43±0.25	2.39±0.19	2.24±0.11
7	2.01±0.11	1.96±0.10	1.90±0.18	2.38±0.24	2.36±0.18	2.10±0.08
8	1.24±0.09	1.33±0.07	1.54±0.14	1.61±0.20	1.62±0.16	1.54±0.07
9	1.81±0.09	1.85±0.08	2.02±0.17	2.33±0.17	2.35±0.17	2.03±0.03
10	5.94±0.25	5.96±0.27	5.43±0.40	7.87±0.65	8.96±0.37	7.60±0.20

^aResults from Ref. 14.

with corrections for target self-absorption and detector efficiency as has been described elsewhere.¹¹ The observed intensities are shown in Table V.

It is apparent that the muonic K -x-ray intensity patterns measured for the iron compounds and solutions differ remarkably for the two groups of targets (see Sec. I). In the first group the intensities for the high members of the K series are relatively low, and in the second, *grasso modo*, high. It is interesting to note that the intensity pattern previously measured for metallic iron¹⁴ appears intermediate between the two groups.

In order to gain greater insight into the angular momentum characteristics of the muons captured in various samples, we fitted the measured x-ray intensities with cascade calculations starting with an "initial" angular momentum distribution $P(l)$ at principal quantum number $n=20$. The cascade program was developed by Hüfner¹⁵ and modified by Hartmann.¹⁶ Distributions of the forms of first- and second-degree polynomials were considered. Table VI shows the parameter of the linear distribution $P(l) \propto 1+bl$ together with the reduced χ^2 values for the two distributions indicating the quality of the fit. The graphical display of both the linear and quadratic angular momentum distributions we have determined for the six systems studied are also shown in Fig. 2. We do not believe that the second-order polynomial yields in general either a markedly better intensity fit or is required by our data.

It is immediately apparent that the first three compounds FeCl₃, Fe₂O₃, and 1.9M Fe(NO₃)₃ belonging to

TABLE VI. Values of fitted muonic angular momentum distributions.

Compound	b	χ_1^2 ^a	χ_2^2 ^b
FeCl ₃	+0.080±0.006	1.89	1.85
Fe ₂ O ₃	+0.075±0.007	2.60	2.04
1.9M Fe(NO ₃) ₃	+0.072±0.009	1.62	1.13
K ₃ Fe(CN) ₆	+0.003±0.005	1.44	0.72
K ₃ Fe(CN) ₆	$b=0$ required	1.32	
1.0M K ₃ Fe(CN) ₆	-(0.006±0.003)	2.40	2.50
1.0M K ₃ Fe(CN) ₆	$b=0$ required	2.56	
Fe metal ^c	0.049±0.005	4.69	4.30

^aFor linear polynomial.

^bFor quadratic polynomial.

^cData taken from Ref. 14.

the first group of targets have indistinguishable cascade angular momentum distributions. The average linear fit parameter $b = +0.076$ indicates that the $l=19$ highest angular momentum states are favored by about 50% over the lowest angular momentum state $l=0$. The angular momentum distributions for the second target group are also very similar to each other but are markedly different from those of the first group. They are almost independent of l , i.e., flat. The distribution required to fit the metallic iron is intermediate between these two compound classes. The distribution parameters confirm the qualitative features already apparent in the intensity data of Table V.

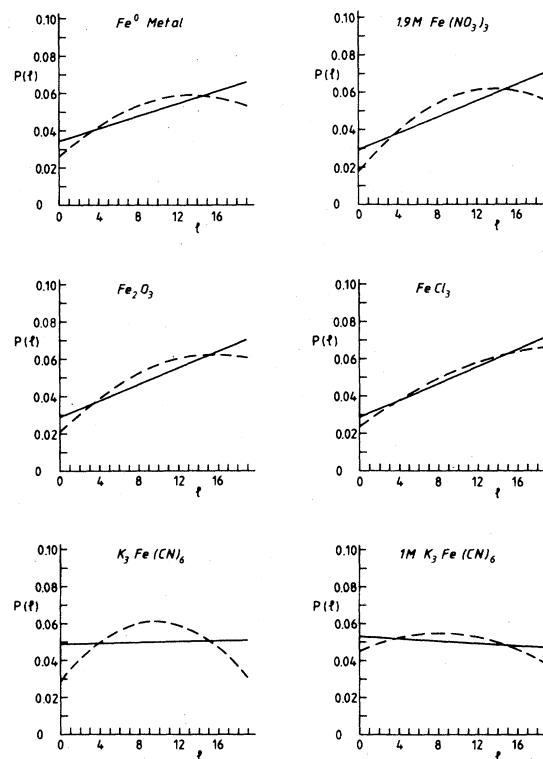


FIG. 2. Angular distribution of the muons at $n=20$ obtained from a fit to the K -series intensities (solid line, linear distribution; dashed line, quadratic distribution).

III. DISCUSSION

The similarity between the patterns of ferric-nitrate solution and the other simple ferric compounds on one hand and those of the potassium ferricyanide in crystal-line form and solution on the other deserves a comment. It has been already noted⁵ from a comparison of the muonic K -x-ray intensity patterns measured for a simple crystalline salt, NaCl, and its aqueous solution that the cation (Na^+) pattern shows little change while the anion (Cl^-) shows a marked enhancement of the intensities of the higher K muonic x rays in the case of the solution. A hydrogen-atom proximity effect, already well-established for compounds containing chemically bound hydrogen atoms, was invoked to explain this effect. It was noted that for simple hydrated anions the hydrogen atoms of the surrounding dipolar water molecules are oriented towards the anion and away from the cation. This picture can explain the negligible difference observed for the 1.9M ferric-nitrate solution where the iron is in cationic form. The lack of a major effect in the case of the ferricyanide anion can also be understood since the hydrogen atoms of the water dipoles are in close proximity to the atoms of the cyanide groups which occlude the central iron atom. The observations for hydrated ions in solution and compounds indicate that the hydrogen atoms probably should be located immediately adjacent to the atom of interest if a strong hydrogen-atom effect is to be observed.

Turning now to the role of the iron electrons, we first recall that the triply ionized iron atom in vacuum (23 electrons) has as its ground-state electron configuration 18 electrons in an argon core plus 5 electrons occupying atomic $3d$ orbitals. Neglecting magnetic splitting, 16 distinct terms can arise from this $3d^5$ electron configuration. In the fourth optical spectrum of iron, five of these terms have been reported: 6S (ground state), 4G , 4P , 4D , and 4F , at respective excitations of 0, 3.97, 4.36, 4.78, and 6.47 eV.¹⁷

In compounds of the metallic transition elements, the number of electrons present in d -related orbitals is the same as the number of d atomic electrons that occur in the corresponding gaseous ion with the same valence charge. The five d -related orbitals of the compound are mainly centered on the metallic atom; they correlate closely with the free-atom d orbitals. For compounds with octahedral bonding of six nearest neighbors, the d -related orbitals consist of a degenerate triplet of states with symmetry classification t_{2g} lying below a degenerate doublet of e_g states.¹⁸

For "weak-field" ferric compounds the splitting between the doublet and triplet states is small and the high-spin configuration $t_{2g}^3 e_g^2$ is lowest lying, leading to an $S = \frac{5}{2}$ ground state. This configuration is supported by magnetic susceptibility data¹⁹ for ferric chloride, high-temperature ferric oxide, and samples containing the hydrated ferric ion.²⁰ The optical-absorption spectroscopy^{21,22} for these weak-field systems involving the Fe^{+3} ion involves transitions to the terms arising from the next higher configuration $t_{2g}^2 e_g^3$.

The "strong-field" iron complex $\text{K}_3\text{Fe}(\text{CN})_6$ involves a much larger energy difference for the t_{2g} and e_g orbitals.

The ground-state configuration assigned is $t_{2g}^5 e_g^0$, i.e., a configuration with one unpaired electron and $S = \frac{1}{2}$. Magnetic susceptibility data²³ are in accord with this assignment; the optical-absorption spectrum for this compound has been interpreted²⁴ with transitions to terms arising from the $t_{2g}^4 e_g^1$ configuration.

The possible connection between systems with open electron inner-shell configurations and special muon-capture features has already been indicated.⁵ We first note that the number of microstates, $N(m)$, arising in an atom or compound when m electrons occupy a group of d -related orbitals ($l=2$) starts to rise rapidly with m and rises until the group is half-filled:

$$N(m) = \frac{(4l+2)!}{(4l+2-m)!m!}$$

Then $N(m)$ falls. For example, for d -related orbitals one has $N(1)=N(9)=10$ while $N(5)=252$. The number of spectroscopic terms similarly increases and decreases symmetrically about the half-filled group. In atoms, for example, a single 2D state occurs if $m=1$ or 9 while the 16 terms occur when $m=5$. For such systems we suggest that one-electron excitations of d -to- d type play an important role in both the muon Coulomb capture and cascade processes. The close similarity between the initial and final radial distributions appears to favor such transitions which enhance the possibility for loss of both muon energy and muon angular momentum. The one-electron transitions suggested involve spatial reorientation of the orbital angular momentum of one d -type electron, i.e., an electron with a markedly higher angular momentum than the s or p electrons encountered in the valence shell of atoms at the beginning or end of each row of the periodic table. The maximum change in the azimuthal quantum number permitted in such a d -to- d transition is $\Delta m_l = 4$. Thus, a single transition of the type we have postulated offers the possibility of a relatively large change in the muon angular momentum provided this particle is interacting with an atomic center containing a partially filled group of d -type orbitals.

The similar features we observe for muon capture in the simple high-spin ferric compounds support the concept that the electron structures of the ionic cores present in these compounds determine the angular momentum characteristics rather than do the nature or distance of the neighboring atoms.

One consequence of the d -to- d excitation mechanism is that the number of such electron transitions should fall beyond the five-electron half-filled d group. A previous publication⁹ from this laboratory has revealed that the experimental muonic x-ray-intensity ratio $I_{K\beta}/I_{K\alpha}$ shows the same systematic variation for a series of metallic $3d$ transition elements and their oxides. The maximum in this ratio is reached for iron and manganese, $Z=25$ and 26, where the half-filled d^5 atomic configuration exists for these atoms or their doubly charged ions.

A possible suggestion for the origin of the differing muon angular momentum characteristics observed for the simple ferric compounds and the ferricyanide samples may also be outlined in terms of the differing d -type electronic structures of these compounds.

TABLE VII. Muon-capture ratios for rare-earth fluorides (experimental data taken from Ref. 25).

	${}_{57}\text{La}^{+3}$	${}_{58}\text{Ce}^{+3}$	${}_{60}\text{Nd}^{+3}$	${}_{64}\text{Gd}^{+3}$	${}_{66}\text{Dy}^{+3}$	${}_{68}\text{Er}^{+3}$	${}_{70}\text{Yb}^{+3}$
$A(M, {}_9\text{F})$	3.93	5.40	6.72	7.29	6.79	6.78	5.05
	± 0.28	± 0.34	± 0.44	± 0.70	± 0.51	± 0.45	± 0.55
m	0	1	3	7	9	10	13

Let us first treat the case of the second group of targets, all with a spin $S = \frac{1}{2}$ in the ground state. For the conjectured d -to- d electron transitions during muon capture and, in particular, cascade there is always an increase of total electron spin S necessary, i.e., the muon delivers angular momentum and hence is shifted to low l states, in accordance with the observation of high intensities of the higher Lyman transitions. For the first target group with $S = \frac{5}{2}$ this argument cannot be applied, in accordance with the observation of lower intensities of the higher Lyman transitions.

The considerations outlined above should also apply to muon capture by metals and compounds of the rare-earth and actinide elements. Here optical and magnetic data show that partially filled, essentially unperturbed, atomic $4f$ or $5f$ electron shells are present.^{20,23}

We have reported measurements of the per-atom muon-capture ratios $A(Z, {}_9\text{F})$ for a series of solid rare-earth trifluorides, MF_3 .²⁵ The electronic structure of the triply charged ionic cores is $\text{Xe} + 4f^m$. It is known that most physical and chemical properties of the rare-earth compounds vary only slightly and in a continuous manner, e.g., the ionic radii of the triply charged ions. As shown in Table VII, however, the capture ratios $A(Z, {}_9\text{F})$ show a steep rise and fall correlating with the number of $4f$ electrons. If f -to- f electronic rearrangement excitations play an important role, the rare-earth ion with seven $4f$ electrons offers the greatest possibility for such transitions. This is indeed the case for gadolinium fluoride. We point out also the similar capture probabilities measured for cerium fluoride and ytterbium fluoride, with one electron and one electron vacancy, respectively, and the profound influence of even a single $4f$ electron reflected in the difference of the capture ratios measured for lanthanum and cerium fluorides.

In summary, the concept of enhanced energy and angular momentum loss from a moving charged particle, the muon, to atomic systems containing an open d - or f -electron configuration has been introduced. The suggestion of d -to- d or f -to- f electron excitations accounts for a number of experimental features encountered in muon-Coulomb-capture studies. Presumably such effects should also be operative in energy-loss mechanisms involving other charged particles. Such behavior has indeed been noted by the Uppsala group in their ESCA (electron spectroscopy for chemical analysis) photoelectron emission studies.²⁶ Photoelectron line shapes have been systematically studied for a number of metals where open and closed d -electron configurations occur. For example, in the sequence iron, cobalt, nickel, and copper a relatively large energy loss was noted for the photoelectrons from iron. The least energy loss was observed for copper metal involving an atomic core with a closed d -shell configuration. These observations are in agreement with the energy-loss mechanisms that we have invoked here.

ACKNOWLEDGMENTS

One of us (R.A.N.) expresses with pleasure his gratitude to the Alexander von Humboldt Stiftung for the generous support provided during two enjoyable stays in Germany which made this work possible. The hospitality and support by SIN is gratefully acknowledged. This work was also supported by the German Bundesministerium für Forschung und Technologie and the United States Department of Energy. We would like to acknowledge the kind assistance of Dr. G. Fottner with these measurements and a most helpful discussion with Professor T. Estle.

*Permanent address: Departments of Chemistry and Physics, Princeton University, Princeton, New Jersey 08544.

¹T. von Egidy and F. J. Hartmann, Phys. Rev. A **26**, 2355 (1982).

²V. G. Zinov, A. D. Konin, and A. I. Mukhin, Yad. Fiz. **2**, 859 (1965) [Sov. J. Nucl. Phys. **2**, 613 (1966)].

³D. Kessler, H. L. Anderson, M. S. Dixit, H. J. Evans, R. J. McKee, C. K. Hargrove, R. D. Barton, E. P. Hincks, and J. D. McAndrew, Phys. Rev. Lett. **18**, 1179 (1967).

⁴Handbook of Chemistry and Physics, 56th ed. (Chemical Rubber, Cleveland, 1975).

⁵R. A. Naumann, J. D. Knight, L. F. Mausner, C. J. Orth, M. E. Schillaci, and G. Schmidt, in *Proceedings of the International Symposium on Meson Chemistry and Mesomolecular Processes in Matter*, edited by V. N. Prokrovskij (Joint Institute for Nuclear Research, Dubna, USSR, 1977).

⁶T. von Egidy, D. H. Jakubassa-Amundsen, and F. J. Hartmann, Phys. Rev. A **29**, 455 (1984).

⁷K. Kaeser, B. Robert-Tissot, L. A. Schaller, L. Schellenberg, and H. Schneuwly, Helv. Phys. Acta **52**, 304 (1979).

⁸C. J. Orth, M. E. Schillaci, J. D. Knight, L. F. Mausner, R. A. Naumann, G. Schmidt, and H. Daniel, Phys. Rev. A **25**, 876 (1982).

⁹T. von Egidy, W. Denk, R. Bergmann, H. Daniel, F. J. Hartmann, J. J. Reidy, and W. Wilhelm, Phys. Rev. A **23**, 427 (1981).

¹⁰H. Daniel, R. Bergmann, G. Fottner, F. J. Hartmann, and W. Wilhelm, Z. Phys. A **300**, 253 (1981).

¹¹F. J. Hartmann, R. Bergmann, H. Daniel, H.-J. Pfeiffer, T. von Egidy, and W. Wilhelm, Z. Phys. A **305**, 189 (1982).

¹²L. F. Mausner, R. A. Naumann, J. A. Monard, and S. N. Kaplan, Phys. Rev. A **15**, 479 (1977).

- ¹³T. von Egidy, H. Daniel, P. Ehrhart, F. J. Hartmann, and E. Köhler, *Z. Phys. A* **308**, 107 (1982).
- ¹⁴F. J. Hartmann, T. von Egidy, R. Bergmann, M. Kleber, H.-J. Pfeiffer, K. Springer, and H. Daniel, *Phys. Rev. Lett.* **37**, 331 (1976).
- ¹⁵J. Hüfner, *Z. Phys.* **195**, 365 (1966).
- ¹⁶F. J. Hartmann (unpublished).
- ¹⁷C. E. Moore, *Atomic Energy Levels*, Natl. Bur. Stand. (U.S.) Circ. No. 467 (U.S. GPO, Washington, D.C., 1952).
- ¹⁸E. Cartmell and G. W. A. Fowles, *Valency and Molecular Structure*, 4th ed. (Butterworths, London, 1977).
- ¹⁹S. Chikazumi, *Physics of Magnetism* (Wiley, New York, 1964).
- ²⁰C. Kittel, *Introduction to Solid State Physics*, 5th ed. (Wiley, New York, 1976).
- ²¹H. L. Schläfer, *Z. Phys. Chem. (Frankfurt am Main)* **4**, 116 (1955).
- ²²M. Dvir and W. Low, *Phys. Rev.* **119**, 1587 (1960).
- ²³D. H. Martin, *Magnetism in Solids* (MIT, Cambridge, Mass., 1967).
- ²⁴C. S. Naiman, *J. Chem. Phys.* **35**, 323 (1961).
- ²⁵F. J. Hartmann, R. Bergmann, H. Daniel, T. von Egidy, G. Fottner, R. A. Naumann, J. J. Reidy, and W. Wilhelm, *Z. Phys. A* **308**, 103 (1982).
- ²⁶Y. Baer, P. F. Hedén, J. Hedman, M. Klasson, C. Nordling, and K. Siegbahn, *Phys. Scr.* **1**, 55 (1970).